# The role of chain length and conformation in stress-transmission and fracture of thermoplastic polymers

© Hans-Henning Kausch-Blecken von Schmeling

Institute of Materials, Swiss Federal Institute of Technology Lausanne (EPFL),
CH-1015 Lausanne, Switzerland

E-mail: hans-henning.kausch@epfl.ch

In this presentation a review of the molecular aspects of fracture is given, a subject that was pioneered by S.N. Zhurkov and his collaborators. Particular attention will be paid to the mechanisms of stress transfer onto straight chain segments, the role of chain interpenetration in establishing interfacial strength during crack healing, to the concept of taut tie-molecules, to stress distribution in UHMWPE fibres, and to the possible role of chain ruptures in the deformation process of fibres. Using Raman microscopy it is observed that some chains are exposed to stresses of up to 10 GPa, which is close to their estimated strength. From these experiments a mechanical model of the organization of almost fully oriented UHMWPE fibres is developed accounting also for the presence of numerous and dispersed defects. The principal deformation mechanisms are chain slippage, crystal plasticity and intra- and intermicrofibrillar slippage.

## 1. Introduction

The great length, large anisotropy and high segmental flexibility of macromolecules give rise to the complex structural organisation and the unique properties of polymer materials. The weak lateral coherence of strong chain segments offers an enormous potential for processing at comparatively low temperatures and it is an essential condition for polymer ductility, rubber elasticity and viscoelastic behaviour. In this presentation we discuss amorphous and semi-crystalline thermoplastics. Their mechanical properties depend on the intensity of the van der Waals attraction between molecular segments, the density of entanglements and on long-range stress transmission by extended chain segments. These characteristics are responsible for the strong effect of time and temperature of macroscopic performance.

The emerging macromolecular science (since the early twenties [1]) rapidly identified the important role of length and conformation of chain molecules in solution [1], in the rubbery state [2] and in solids [3]. From the many and important discoveries and concepts made in the following three decades we may cite the new methods of synthesis controlling the stereoregularity of chains (Ziegler/Natta), the decisive theoretical work on chain conformation and statistical thermodynamics (e. g. W. Kuhn/H. Kuhn/ Flory/Volkenstein/Rouse), the surprising discovery of the chain-folded lamellar structure of semi-crystalline polymers (Fischer/Keller/Till), and the better understanding of (ultimate) mechanical properties such as the formation and microstructure of crazes (Kambour/Hsiao/Sauer), of the nature of elementary deformation mechanisms (Eyring/Wolf/Schmieder/Heijboer) and of the essential parameters of time-dependent polymer fracture (Tobolsky/Zhurkov/Bueche). These so exiting Origins and growth of polymer science have been competently reviewed by Morawetz [4].

In fracture through crack propagation of a solid polymer, chains must be disengaged from each other across the fracture plane. In thermoplastic solids, where chains cohere through van der Waals forces, this involves several terms, which all depend on the stress transfer through and the breaking of secondary bonds. The relative contributions of the different mechanisms are well reflected by the fracture energy $G_{Ic}$ plotted in Fig. 1 as a function of chain length (molecular weight).

Using an unoriented amorphous thermoplastic such as polymethyl methacrylate (PMMA) as an example it is well seen, that the separation of very small molecules (low $M_W$ material) only requires work against the intermolecular attraction, since $G_{Ic}$ is equivalent to two times the surface tension parameter $\gamma$. In the following region $G_{Ic}$ shows a moderate and linear increase with $M_W$, which indicates that the pull-out of chains from a rather restricted fracture surface zone contributes to the dissipation of energy. Once the chains are long enough to form entanglements, energy dissipation (by plastic deformation and/or crazing) is spread out into a larger volume element leading to a strong increase of $G_{Ic}$. Understandably, in a solid, where cohesion occurs

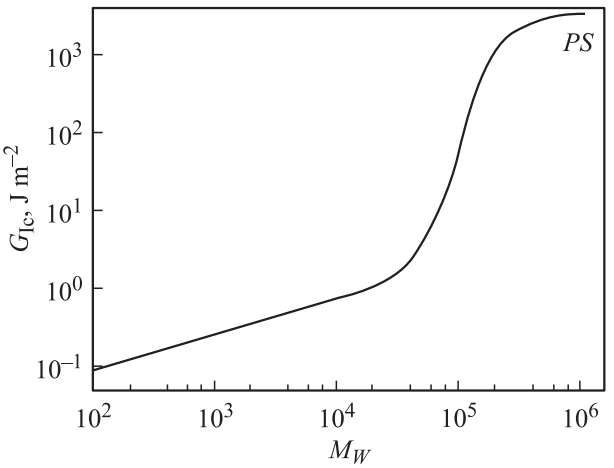


**Figure 1.** Energy release rate $G_{Ic}$ as a function of chain length ($M_W$) for poly(methylmethacrylate) (PMMA).

more or less exclusively through the lateral van der Waals interaction between chain segments, the fracture energy levels off for very long chains. For PMMA a terminal value of $G_{Ic}$ of about $300\,\mathrm{Jm}^{-2}$ has been determined, which is several orders of magnitude smaller than the fracture energy of a mono-crystal, where primary bonds are loaded and broken [5]. (It should be noted that in that case most of the fracture energy is loss of elastic energy when the highly loaded chains are discharged, the chemical surface energy of breaking primary bonds (chain scission) is — compared with the elastic term — rather small, for most polymers it is of the order of 0.4 to $3\,\mathrm{Jm}^{-2}$ [5]). It may be mentioned that a rather weak dependence of chain length is also obtained for the elastic and anelastic properties of glassy polymers, which are cohesive in nature.

A much stronger effect of chain length is found, however, under experimental conditions, which permit the (partial) unfolding of the coiled chains: in solution, in highly oriented polymers and/or with properties involving larger strains or time to failure. Under such conditions notable axial stresses can be transferred onto the chain backbone greatly improving the overall load bearing capability. In the pioneering work done at the Ioffe Physical Technical Institute in the then Leningrad S.N. Zhurkov and his collaborators have attacked this problem, namely to identify molecular deformation and/or damage mechanisms in order to understand the kinetics of polymer breakdown. In referring to their work we discuss in this paper the micro-mechanics of stressed samples due to the action of (and the competition between) different mechanisms: conformational changes, segmental slip, disentanglement, chain stretching and scission, and void and/or micro-crack formation. The strongly time- and temperature-dependent dynamics of these mechanisms determines the modes of deformation and fracture (through e.g. crazing, shear yielding, creep and/or crack propagation). For this purpose we will study two quite different systems: the fracture (and crack healing) behaviour of amorphous polymers (PMMA, SAN) and the ultimate properties of highly oriented ultra high molecular weight polyethylene (UHMWPE).

## 2. Early studies at the Ioffe Physical Technical Institute

In order to elucidate the molecular origins of polymer fracture Zhurkov and his collaborators have used — and in part developed — a variety of experimental and theoretical techniques. Their fruitful activity has given rise to several hundreds of original publications (initially mostly in Russian). Much of this work has been reviewed in two relevant monographs: Fracture Micromechanics by Kuksenko and Tamusz [6] and Polymer Fracture by Kausch [5].

The author of this paper had first become acquainted with the Leningrad investigations by Zhurkov's presentation at ICF1 in Sendai in 1965 [7], where he reported that the time to failure $\tau$ of a sample under tensile stress $\sigma$ could be well described by one general kinetic equation valid for quite different polymers

$$\tau = \tau_0 \exp\left(\frac{U_0 - V\sigma}{kT}\right), \tag{1}$$

where $k$ is Boltzmann's constant and $\tau_0$, $U_0$ and $V$ are constants determining the strength characteristics of a polymer. From his experiments he had determined that the activation energy $U_0$ of mechanical fracture compared well with the activation energy for thermal destruction. The pre-exponential term $\tau_0$ was roughly the same for all polymers studied and of the order of $10^{-12}$ to $10^{-13}$ s. Similar relationships between stress and mechanical properties had been proposed independently by Tobolsky–Eyring (creep rate) and Bueche (lifetime) [5].

In order to learn more about the micro-mechanics of a stressed system formed of weakly cohering strong chain backbones the Zhurkov team followed a remarkably broad approach using techniques, which were then applied for the first time to such systems.

Axial forces transmitted to an extended elastic tie-chain segment stressed between two crystalline lamella were calculated [8].[1]

Stress effects on chain segments were theoretically analyzed and experimentally determined quantitatively from the shift and deformation of infrared (IR) bands of characteristic skeleton vibrations with applied load [9].

Scission of chains was traced through the accumulation of free radicals by electron spin resonance technique (ESR) [10]. Thus for the first time direct evidence was presented on stress-induced homolytic chain scission during the loading of polyamide 6 (PA6) and natural silk. In ruptured specimens the concentration of free radicals amounted to about $5 \cdot 10^{18}\,\mathrm{cm}^{-3}$ (which in this case is about twice the number of broken chains). In view of the small loads transmitted to the axes of statistically coiled chains most of the above ESR and IR experiments were performed with oriented films or fibres.

Following chain scission new, oxygen-containing groups were formed and could be determined quantitatively by IR technique [11].

Micro-cracks appearing in stressed samples were studied by small angle $x$-ray scattering [12].

Strong synergisms and similarities were detected between the kinetics of mechanical and electrical breakdown [13].

These intriguing experiments had stimulated the research in this area in other parts of the world, with ESR and IR investigations notably done in Salt Lake City [14] and Darmstadt [15]. They gave undisputed proof that during straining and fracture chain segments had been loaded up to scission. A quantitative analysis showed that the number of the highly stressed segments was small, increasing with the degree of molecular orientation. Even in highly oriented

[1] The references [8] to [13] are among the first publications on these particular subjects available in English, they are not meant to provide a comprehensive coverage of the activities of the Zhurkov laboratory.

fibers no more than between 3 and 5% of all segments were overstressed [5,6]. In the following we will indicate the molecular and experimental parameters favouring the stress-transfer onto (extended) chain segments and discuss more recent techniques, the crack healing approach, the compatibilization using block copolymers, and bond stress analysis by Raman microscopy, techniques employed to obtain direct information on the role of chain backbones in fracture of polymers.

## 3. Stress-transfer onto extended chain segments

All axial chain stresses derive from the relative displacement of chain segments with respect to their surrounding. It is useful to distinguish between static and dynamic stress transfer. The axial stress $\psi_i$ resulting from the static displacement of a straight, elastic linear chain segment against a sinusoidal interaction potential (modelling the repulsive forces a monomer unit encounters within a PE crystal) was first calculated by Chevychelov [8]; Kausch and Langbein [16] later extended these calculations to interaction potentials in the presence of hydrogen bonds (as in the lamellae of PA6). In both approaches the maximum chain tension is proportional to the product of potential depth and chain elasticity. The forces thus obtained amounted to 1.4 nN (PE) and 4 nN (PA6) respectively [5,8,16].

In the dynamic case a stress $\psi_i$ is transferred upon a straight segment of finite length $L_i$ by friction

$$\psi_i = \xi_0 \dot{\delta}_0 L_i, \qquad (2)$$

where $\xi_0$ is the monomeric friction coefficient and $\dot{\delta}_0$ is the rate of segment displacement (e.g. during chain pull-out). Stresses will obviously be the higher the more regular and longer a segment is (absence of kinks or other irregularities capable of relaxing axial stresses by simple change of conformation) and the closer such an extended stiff segment is oriented into the principal stress direction. Small rates of loading and high temperatures as well as all modes of intra- or inter-segmental relaxation will decrease the attainable level of axial stresses — and for that matter — contribute to the toughness of a specimen (see [17] for an extended discussion of the effect of molecular mobility on toughness). A comprehensive molecular analysis of the static and dynamic loading of chains at interfaces and of their influence on the mode of failure has recently been given by Creton et al. [18].

Stress distribution on isotropic semi-crystalline polymers is dominated by the large stiffness differences between amorphous and crystalline regions. The presence, phase structure, quality and organization of the crystalline lamellae strongly influence all mechanical properties [19,20]. Within the context of this presentation particular attention must be paid to tie-molecules. Anchored in adjacent lamellae the tie-molecules (and/or crystalline bridges) are capable of efficient stress-transfer, which is absolutely essential to attain high levels of stiffness and strength. Tie-molecules bear high load, they are the first to be overstressed and scissioned. Evidently the direct study of stress effects on chain segments is best performed on highly oriented (film or fibre) specimens as this has been done so successfully at the Ioffe Institute [7–13,21–27].

## 4. Stress transfer in amorphous polymers

4.1. Crack healing. The stress transmission by chain backbones in amorphous polymers can be most conveniently studied using the crack healing approach; conceived and developed by Jud, Kausch and Williams [28], Wool [29], Brown et al. [30] and Kramer et al. [18] it consists in the determination of the gradual build-up of interfacial strength through chain interdiffusion between two flat surfaces of identical (or compatible) amorphous polymers brought into contact at a temperature above the glass transition $T_g$. The term crack healing had been chosen to differentiate this slow and time-dependent approach from welding of semi-crystalline thermoplastics, which involves the fusion and — often rapid — reformation of crystal lamellae. (The physical particularities of the welding technique, especially the advantages of non-isothermal welding, have been extensively investigated by Manson's laboratory in Lausanne, see [31,32] for more references). To determine the strength restored to healed or welded surfaces appropriate fracture mechanics specimens were used and fracture toughness $K_{Ic}$ or fracture energy $G_{Ic}$ were taken as a mesure of interfacial strength.

The experiments with (compatible) amorphous polymers [5,18,28–30] confirmed that the sequence of physical events in strength build-up is the following: establishment of (partial) mechanical contact between surfaces, surface reorganization, full contact, interpenetration of segments across the interface at a rate determined by compatibility of the interdiffusing species, chain mobility and mechanical constraints, further interpenetration of whole chains and successive formation of entanglements; semi color at rather long times the former interface will have disappeared completely.

Using the reptation model of de Gennes [33], Kausch et al. [28,34] and Wool [29,35] have proposed kinetic models of strength build-up in crack healing based on the formation of new entanglements. Due to the statistical nature of the process of chain diffusion by reptation there will be a large local variation of the number of diffusing chain ends and of the curvilinear depth $\Delta u$ of their interpenetration. This means that even at small values of $(\langle \Delta u^2 \rangle)^{1/2}$ there are some chains, which have penetrated much further than the minimum distance $\Delta u_{\min}$ necessary to form an entanglement. During the crack healing process $n(t_h)$ new entanglements per unit surface area are formed in the interfacial region near the former crack surfaces. Unless the healing has been absolutely complete, $n(t_h)$ will be smaller than $n_e$, the corresponding concentration of entanglements

in the virgin material. The wriggling and translational motions of the chain segments within their confinement, the so-called tube, give rise to an average curvilinear displacement $\Delta u$ of the chain ends which is described by the Einstein relation

$$\langle \Delta u^2 \rangle = 2D_t t_t. \quad (3)$$

Following the argumentation of the above authors that the fracture energy $G_c(t)$ of the healed interface is proportional to the number of entanglements formed, a relation between stress intensity factor $K_c$ measured after healing and healing time $t_h$ is obtained

$$K_{c,rel} = \frac{K_c}{K_{I_0}} = \left(\frac{G_c}{G_{c_0}}\right)^{1/2} = \left(\frac{n(t_h)}{n(\tau_0)}\right)^{1/2} = \left(\frac{t_h}{\tau_0}\right)^{1/4}, \quad (4)$$

where $K_{10}$ and $G_{c0}$ refer to the virgin material, $\tau_0$ is the time necessary for complete healing. It is this equation, which has explained for the first time and in a straightforward manner the $t^{1/4}$ dependence of the increase of the stress-intensity factor with healing time as it had been observed in amorphous PMMA and SAN [28,29].

Despite the quite satisfactory explanation of the time dependence of crack healing it must be noted that the assumptions made in deriving the above model have led to the elimination of $D_t$ from the final formula. Thus the above model does not account for a number of parameters, which have been shown to influence the strength build-up in a healing interface such as: the absolute values of $D_t$ or of the critical distance of interpenetration at complete healing, the nature of the diffusion mechanism (by reptation of the chain ends or by displacement of hairpin segments?), the absolute number of involved connector chains or the number of connections per chain.

Such information was obtained by Kramer, Creton and Brown et al. in their elegant interdiffusion experiments using the compatibilization between two incompatible polymers by appropriately chosen block-copolymers (reviewed in [18,30]). The principle of this technique and some results are presented in the following Section.

4.2. Use of block copolymers to count molecular connectors. The principle to use block copolymers as compatibilizing agents is straightforward. Two incompatible polymers $A$ and $B$ will generally form a clearly phase separated system. Figure 2 shows as an example a thin film of a blend of 10% polysulfone (PSF) particles dispersed in an (incompatible) polystyrene (PS) matrix. The interfaces between the two components are sharp and well defined. When such a film is deformed, large crazes open up in the matrix.

The interior of the craze is characterised by a larger number of defects: local ruptures of craze fibrils which originate without exception at the surface of the PSF particles betraying the rather weak van der Waals attraction between the incompatible polymer pair PS–PSF. Such a PS–PSF blend can be compatibilized by adding a (PPO–PSF) tri-block copolymer to it. The blocks will interdiffuse into

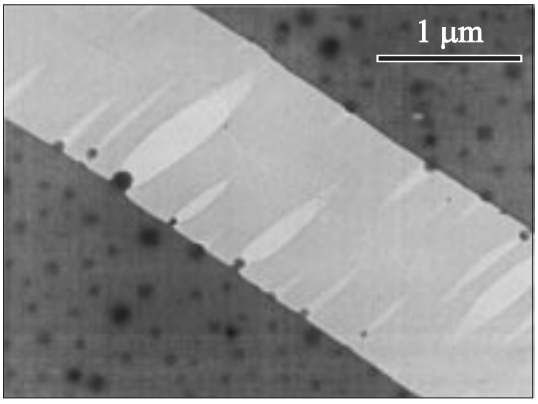


**Figure 2.** Craze in a thin film of an incompatible blend (10% PSF particles in a PS matrix) deformed at room temperature (after [34]).

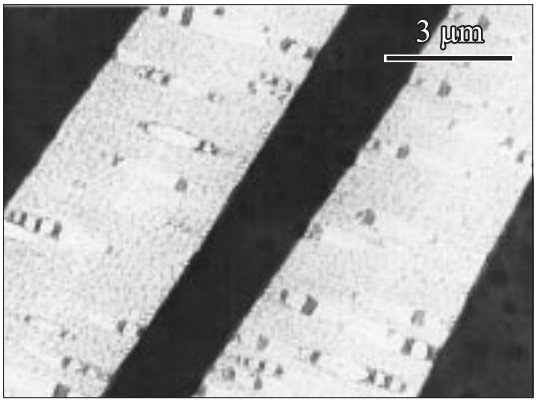


**Figure 3.** Craze in a compatibilized blend (11% free PSF particles in a PS matrix, PPO–PSF tri-block copolymer as compatibilizer) (after [34]).

the phases with which they are compatible: the two PPO end-blocks into the PS matrix, the central PSF block into the PSF particles. From this interdiffusion result two strong covalent bonds per molecule having penetrated the interface. Assuming the force transmitted by each bond to be $f_0$ and their surface density to be $\Sigma$ the following interfacial strength $\sigma$ is obtained:

$$\sigma = f_0 \Sigma. \quad (5)$$

As evidenced by Fig. 3 the interfacial strength $\sigma$ can be higher than the crazing strength of the PSF particles so that the latter break up when the matrix craze is formed or extended.

The essential parameters controlling the interfacial strength of a compatibilized blend are evidently the number of covalent ties at the particle surface and the strength with which a block is anchored in its respective phase (which depends on block length). In their early quantitative experiments on the build-up of interfacial strength through block copolymers Brown et al. [18,19] create a strong interfacial bond between two flat slabs of respectively

PMMA and PPO by interdiffusing an interlayer of a PMMA–PS diblock copolymer. Each diblock thus provides a covalent bond between the slabs. These experiments have permitted for the first time to virtually count the number $N_{di}$ of primary bonds joining the two slabs. Using marked molecules, the authors [18,30] have also proven the fact that the PMMA section of the diblock interdiffuses only into the PMMA slab and the PS section only into the PPO. This way they are assured that the number of main chain crossings at the interface must be equal to the number $N_{di}$ of diblock chains available at the interface. For a given thickness of the diblock interlayer — e. g. 25 nm — the number $N_{di}$ obviously decreases with the $M_W$ of the diblocks. As it turns out the fracture energy of the interdiffused slabs reaches saturation values for the $282\,k$ [2] and $355\,k$ material with $N_{di}$ values of 22 and $17.5 \cdot 10^{16}\,\mathrm{m}^{-2}$. The latter crossing densities are only 15 and 12% respectively of the maximum crossing density theoretically permitted by the chain cross-section. With the largest molecular weight the crossing density even drops to 5%. This is evidently equivalent to saying that one needs only relatively few, well-anchored chains crossing a given interface in order to achieve full mechanical interfacial strength. This result is in line with the earlier conclusions based on the ESR and IR experiments [5,9–11]. It also confirms the observation, that the presence of some 5 to 10% of high moleuclar weight material has a beneficial effect on the long term and fatigue strengths of thermoplastics (see [5] for references).

## 5. Ultra high molecular weight polyethylene (UHMWPE) fibres

5.1. Modellization of Micro-structure. In the previous Section we have indicated that the stiffness and strength of linear molecules can be utilized maximally if all soft and misaligned segments are eliminated. A perfectly organized and strong (but also quite brittle) system would be an all-trans mono-crystal such as poly(diacetylene), which has a strength $\sigma_b$ of up to 1.5 GPa. Highly oriented (semi-crystalline) fibres generally retain some non-crystalline material, which is at the origin of the important flexibility without reducing fibre strength ($\sigma_b$ of UHMWPE may reach up to 7 GPa). In our experiments we have used SK60 fibres,[3] which consist of 117'000 macro-fibrils each having a diameter of 0.2 to 2 $\mu$m [36]. They are highly ordered but not mono-crystalline. From measurements of fibre crystallinity and density it can be concluded that there is a fraction of about 25% of non-crystalline material. This fraction comprises highly extended but non-crystalline segments (having a density of 0.90 g/ml), the rare entanglements (about 2.5 per molecule) and folds. The NMR-amorphous phase is accounting for less than 5% of the material; the absence of an amorphous $X$-ray halo indicates an even smaller fraction. The above data show that the amorphous component cannot be expected to form a coherent phase, more likely it comprises all the less ordered segments, tie molecules, conformational irregularities (out of register, twists, rare entanglements) and defects in the crystalline phases and at the boundaries and interfaces of micro-fibrils. From these findings a two-dimensional model of the studied SK60 fibres is proposed (Fig. 4). Basically this model is valid for most highly oriented fibres, although it should be noted that the detailed morphology depends on the starting material (chain length and linearity, degree of entanglement, crystalline morphology) and on the applied processing technique (solid state or melt extrusion, gel spinning, hot drawing) [22,25,37,38].

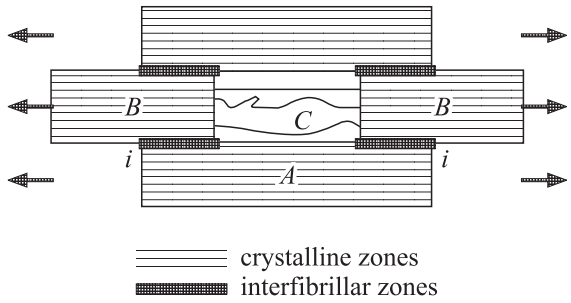


**Figure 4.** Two-dimensional mechanical model of a macrofibril of UHMWPE showing the essential structural elements: crystalline regions, inter-microfibrillar zones, and non-crystalline regions containing more or less taut tie-molecules (the possible slight misalignments, distortions, and variations in width of microfibrils are not shown; see text for the size of the crystalline regions) (after [36]).

The regions $A$ and $B$ represent fully chain-extended crystalline regions (having an elastic modulus of 290 GPa). Phase $C$ describes the fraction of about 25% of slightly desordered non-crystalline chain segments (most of which are well extended). It is reasonable to assume that this phase contains intra-microfibrillar tie-molecules of various degrees of taughtness. The tie-molecules are capable to transmit important axial stresses (the pull-out stress of a tie-molecule from a defect-free orthorhombic crystal amounts to 7.5 GPa [16]). Stresses between the crystalline blocks $B$ are also transferred by shear through the interfaces $i$ and region $A$. Concerning the size of the crystals in UHMWPE-fibres, the lateral dimensions were found to decrease with draw ratio to a value of about 13 to 15 nm [27,36]; the crystalline lengths in chain direction, however, seem to depend strongly on the fibre type, values of 5 to 71 nm have been reported, which agree quite well with the distribution of straight chain lengths determined by Marikhin et al. by longitudinal acoustic mode spectroscopy (LAM) [26], who obtained a range of 7 to 60 nm.

5.2. Molecular stress analysis. The subject of molecular stress analysis is highly intriguing. More than 40 years ago Zhurkov, Vettegren et al. [9] started to analyze the stress-induced deformation of IR absorption bands and to interpret the obtained results in the frame of the kinetic

[2] $282\,k$ designates a sample with molecular weight $M_W = 282$ kg/mol.
[3] Dyneema®, DSM.

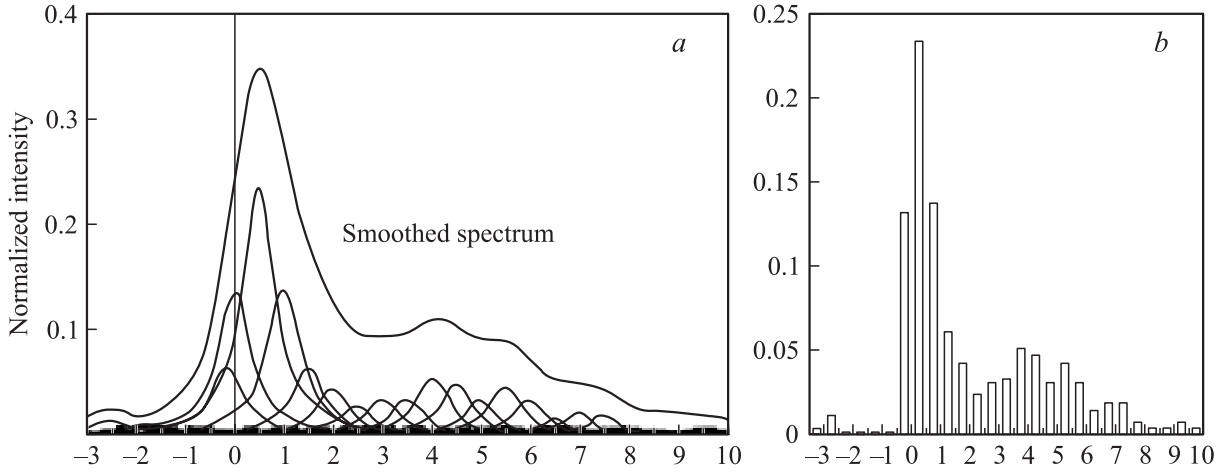


**Figure 5.** Stress analysis of a single filament containing some 150 macrofibrils loaded to a uniaxial stress of 2 GPa: Using a peak shift value of $-5.73\,\mathrm{cm}^{-1}$/GPa the wave number axis is converted into a stress axis ($a$) and subsequently deconvoluted into a stress histogram by curve fitting with some 20 Lorentzian peaks ($b$) (after [36]); the histogram has a clearly bimodal structure.

theory of fracture. Much of their work has been reviewed in the cited books [5,6] or more recently in [23,24]. Evidently it is important to realize that infrared techniques (even Raman microscopy) always scan a volume area, which contains much more than a million of stressed bonds. The seen bonds may be stressed quite differently (this has been recognized in the subsequent stress analysis by fitting a deformed band by some 20 Lorentzian peaks). Secondly it must be understood that (at room temperature) mechanical stress and thermal vibrations contribute to the final fracture of such an overstressed region; as outlined by all these authors in their discussion of the physical nature of the activation parameters in the kinetic equation (1), thermal and mechanical energy of bond rupture can substitute each other. Thirdly, the reader is reminded that the existence and breakage of overstressed regions (in the following simply called bonds or segments) is in itself not yet proof that the strength of oriented polymers is controlled by the scission kinetics of primary bonds.

Molecular stresses were determined by Raman microscopy using the stress-induced shift of the position and form of Raman bands assigned to C–C stretching vibrations [9,36,39]. In polyethylene, the bands at 1060 and $1130\,\mathrm{cm}^{-1}$ exhibit the greatest peak shift upon mechanical deformation. In our investigations we have used the symmetric stretching band at $1130\,\mathrm{cm}^{-1}$, for which we have determined a peak shift value of $-5.73\,\mathrm{cm}^{-1}$ GPa [36]. Using this shift factor the wave number axis of a deformed band can be converted into a stress axis (Fig. 5, $a$). The subsequent transformation into normalized stress intensities is generally achieved by fitting the deformed Raman band by a number of (two or three) Lorentzian peaks [37]. In our approach we have used about 20 Lorentzian peaks having a width corresponding to the width of the peak of an undeformed sample, and which were separated on the converted wave number axis by 0.5 GPa from each other (Fig. 5, $b$).

In the above spectrum most segments are loaded to between 0 and 1 GPa, about one fourth of the population to between 1.5 and 4 GPa and 2.5% to stresses between 5 and 10 GPa. Berger et al. have investigated the changes in local stress distribution occurring in the three loading modes creep, stress relaxation and loading at constant strain rate [36]. Their results are summarised in the following.

Creep loading: The number of weakly (0–1 GPa) and of highly loaded segments (4.5–10) increases at the expense of segments loaded with moderate overstress (1.5–4 GPa), which reinforces the bimodal character of the distribution shown in Fig. 5. This observation can be explained on the basis of the structure model in Fig. 4. The increase in highly stressed bonds is assigned to an increase in the number of taut intra-micro-fibrillar tie molecules during elongation of the fibre (due to the separation of phases $B$) or of taut inter-micro-fibrillar ties (following inter-micro-fibrillar slip). The decrease of moderately overstressed bonds in these fibres is apparently due to the limitation of elastic strain in region $A$, due to slip at the interfaces $i$ or to crystal plasticity. The latter mechanisms would also explain the large and instantaneous variation of creep rates observed by Myasnikova et al. [40,41].

During stress relaxation a decrease of the number of moderately and highly overstressed chains is observed whilst the fraction of less highly loaded material increases. The strong loss in the 5–8 GPa group is ascribed to tie-chain pull-out, the decrease of the moderately overstressed chains to crystal plastic deformation. Both mechanisms are compatible with the observation that even in the stress relaxation mode a large group of crystals remain subjected to a critical strain of about 0.4% [36].

In a tensile test most of the material is never loaded to more than about 1 GPa. Evidently the number of moderately and highly loaded chain segments increases when the applied stress is increased. It should be noted that beyond an external stress of 1 GPa the combined number

of segments stressed at 0.5 and 1 GPa remains relatively constant and accounts for the low stress peak found by other researchers [42].

The possible influence of chain scission had been investigated by Wang et al. [43]. Using a nitroxide spin trap interdiffused into an SK60 fibre they determined that during creep at half the breaking stress 0.2 chain scission events per cm of molecular length occurred. This means that only 1 out of 550 molecules was broken in the experiment. The analysis is the same as given by Kausch [5] for the ESR-investigations of polyamide fibres, namely that chain scission is the *consequence* of stress-induced deformation — but not its cause.

## 6. Final remarks

The molecular aspects of fracture have been reviewed in the light of the seminal work of S.N. Zhurkov and his collaborators. Although stress transmission in thermoplastic polymers occurs exclusively by secondary bonds (even entanglements are loaded that way) chain length, conformation and strength are important parameters. The highest values of sample strength are obtained with highly oriented systems. Polydiacetylene mono-crystals composed of perfectly oriented, *strongly interacting* chains, have a high strength, but they are also brittle because too defect-sensitive. For technically required toughness, it is desirable that at very high stress level local modes of *plastic* deformation are activated, such as chain straightening by elimination of gauche bonds and chain slippage. Both mechanisms can only be active if there is a certain distribution of chain conformations and of local chain stresses. Using Raman microscopy we have demonstrated that in highly oriented UHMWPE fibres some regions are exposed to stresses of up to 10 GPa, which is close to the estimated chain strength. Based on the concept of taut tie-molecules a model of the organization of almost fully oriented UHMWPE fibres has been developed accounting for the numerous and dispersed defects, which are present even in a 99% oriented fibre. Deformation of such fibres occurs by elastic stretching and aligning and straightening of backbones, crystal plasticity and intra- and inter-*micro*fibrillar slippage. To reduce the effect of the latter on the creep properties of the fibres, cross-linking of the molecules and/or incorporation of side groups are appropriate means of modification.

The author wishes to thank his colleagues from the Ioffe Institute for a fruitful and pleasant exchange of arguments, manuscripts and visits for more than 30 years now.

## References

[1] H. Staudinger. Ber. Dt. Chem. Ges. **57**, 1203 (1924).
[2] W. Kuhn. Kolloid-Z. **68**, 2 (1934).
[3] P. Flory. Principles of Polymer Chemistry. Cornell Univ. Press, Ithaca (1953).
[4] H. Morawetz. Polymers, The Origins and Growth of a Science. J. Wiley & Sons, N.Y. (1985).
[5] H.H. Kausch. Polymer Fracture. 2nd ed. Springer, Heidelberg–Berlin (1987).
[6] V.S. Kuksenko, V.P. Tamuzs. Fracture micromechanics of polymer materials. Martinus Nijhof Publishers, The Hague (1981).
[7] S.N. Zhurkov. Int. J. Fracture Mechanics **1**, 311 (1965).
[8] A.D. Chevychelov. Polymer Science USSR **8**, 49 (1966).
[9] S.N. Zhurkov, V.I. Vettegren, I.I. Novak, K.N. Kashintseva. Doklady Akad. Nauk SSSR **176**, 623 (1967).
[10] V.A. Zakrevskii, E.E. Tomashevskii, V.V. Baptizmanskii. Sov. Phys. Solid State **9**, 1118 (1967).
[11] S.N. Zhurkov, V.E. Korsukov. J. Polymer Sci., Polmer Phys. Ed. **12**, 385 (1974).
[12] S.N. Zhurkov, V.A. Zakrevskii, V.E. Korsukov, V.S. Kuksenko. Sov. Phys. Solid State **13**, 1680 (1972).
[13] V.R. Regel, A.I. Slutsker. Transactions of the St. Petersburg Academy of Sciences for Strength Problems **1**, 226 (1997).
[14] D.K. Roylance. PhD dissertation. Univ. of Utah (1968).
[15] J. Becht, H. Fischer. Kolloid. Z.Z. Polym. **229**, 167 (1969).
[16] H.H. Kausch, D. Langbein. J. of Polymer Science: Polymer Physics Edition **11**, 1201 (1973).
[17] Molecular mobility and toughness of polymers / Ed. H.H. Kausch. Adv. in Polymer Science (2005), in press.
[18] C. Creton, E.J. Kramer, H.R. Brown, C.-Y. Hui. Adv. in Polymer Science **156**, 53 (2002).
[19] D.T. Grubb. Chapt. 7 in „Materials Science and Technology: A Comprehensive Treatment“ / Eds R.W. Cahn, P. Haasen, E.J. Kramer. Vol. 12: *Structure and Properties of Polymers* / Ed. E.L. Thomas. VCH, Weinheim–N.Y. (1993).
[20] H.H. Kausch, R. Gensler, C. Grein, C.J.G. Plummer, P. Scaramuzzino. J. Macromol Sci. (1999). B38: 803.
[21] K.J. Friedland, V.A. Marikhin, L.P. Myasnikova, V.I. Vettegren. J. of Polymer Science: Polymer Symp. **58**, 185 (1977).
[22] V.A. Marikhin. Acta Polymerica **30**, 507 (1979).
[23] S.V. Bronnikov, V.I. Vettegren, S.Y. Frenkel. Adv. in Polymer Science **125**, 103 (1996).
[24] V.I. Vettegren, A.D. Gabaraeva, N.L. Zaalishvili. Polymer Science Ser. A **43**, 608 (2001).
[25] L.P. Myasnikova, V.A. Marikhin, E.M. Ivan'kova, P.N. Yakushev, J. Macrom. Science-Physics **40B**, 473 (2001).
[26] V.A. Marikhin, L.P. Myasnikova, E.S. Tsobkallo, V.V. Vasilieva, J. Macrom. Science-Physics **42B**, 939 (2003).
[27] P.M. Pakhomov, S. Khizhnyak, H. Reuter, V. Galitsyn, A. Tshmel. Polymer **44**, 4651 (2003).
[28] K. Jud, H.H. Kausch, G.J. Williams. J. Mater. Sci. **16**, 204 (1981).
[29] R.P. Wool, K. Connor. Appl. Phys. **52**, 5194 (1981).
[30] H.R. Brown. Annual Rev. of Mater. Sci. **21**, 463 (1991).
[31] J.-E. Zanetto, C.J.G. Plummer, P.-E. Bourban, J.-A.E. Månson, J. Hilborn. Polymer **39**, 5939 (1998).
[32] H.H. Kausch, P.-E. Bourban, J.-A. Manson, C.J.G. Plummer. PPS 18. Guimaraes, Portugal (2002).
[33] P.G. de Gennes. Scaling concepts in polymer physics. Cornell Univ. Press, Ithaca (1979).
[34] H.H. Kausch, J. Hilborn, C.J.G. Plummer. Mittal-Festschrift / Eds W.J. van Ooij, H.R. Anderson Jr. VSP (1998). 702.

[35] R.P. Wool. Polymer Interfaces: Structure and Strength. Hanser Publishers, Munich–Vienna–N.Y. (1995).
[36] L. Berger, H.H. Kausch. Polymer **44**, 5877 (2003).
[37] R.S. Porter, L.H. Wang. J. Macromol. Sci.-Rev. Macromol. Chem. Phys. C **35**, 63 (1995).
[38] G.K. Elyashevich, E.A. Karpov, O.V. Kudasheva, Eyu Rosova. Mechanics of Time-Dependent Materials **3**, 319 (1999).
[39] R.J. Young. In: Polymer spectroscopy / Ed. A.H. Fawcett. Chichester, Wiley (1996).
[40] L.P. Myasnikova, V.A. Marikhin, E.M. Ivan'kova, P.N. Yakushev. J. Macrom. Science-Physics **38B**, 859 (1999).
[41] V.I. Vettegren, V.A. Marikhin, L.P. Myasnikova, E.M. Ivan'kova, P.N. Yakushev. Techn. Phys. Lett. **29**, 848 (2003).
[42] J.A.H.M. Moonen, W.A.C. Roovers, R.J. Meier, B.J. Kip. J. of Polymer Science: Polymer Physics Edition **30**, 361 (1992).
[43] D. Wang, A.A.K. Klaassen, G.E. Janssen, E. de Boer, R.J. Meier. Polymer **36**, 4193 (1995).